A regressor-based hysteresis formulation for the magnetic characterisation of low carbon steels

Anastassios Skarlatos, A. Martínez-De-Guerenu, Roberto Miorelli, A. Lasaosa, Christophe Reboud

A regressor-based hysteresis formulation for the magnetic characterisation of low carbon steels

A. Skarlatos[a], A. Martínez-de-Guerenu[b,c], R. Miorelli[a], A. Lasaosa[b,c], C. Reboud[a]

[a] *CEA, LIST, CEA Saclay, Gif-sur-Yvette F-91191, France*
[b] *CEIT, Manuel Lardizabal 15, 20018 Donostia / San Sebastián, Spain*
[c] *Universidad de Navarra, Tecnun, Manuel Lardizabal 13, 20018 Donostia / San Sebastián, Spain*

Abstract

In this work, two different parametric hysteresis models, the Jiles-Atherton model and the Mel'gui relation, have been combined to form a more general hysteresis operator, suitable for the description of families of experimental B(H) curves obtained for low carbon (LC) steel specimens after isothermal annealing at different temperatures and times. As it has been demonstrated in a number of previous studies, characteristic values of steel hysteresis curves can be used as very efficient identifiers for the monitoring of the different metallurgical transformations that take place during the annealing, such as recovery and recrystallisation processes. It is thus important from a practical point to be able to reproduce the experimental curves obtained under different conditions, as precisely as possible, in order to proceed to the samples characterisation. Hybridisation of the two aforementioned models demonstrated satisfactory results for the reproduction of all considered curves obtained under the different considered annealing conditions.

Keywords: hysteresis, parametric models, regression, identification, steel microstructure, isothermal annealing

1. Introduction

Different parametric models have been proposed in the literature for the modelling of magnetic hysteresis, yet none of the existing models proves to be, to the authors knowledge, universal. In fact, a specific model may be well adapted for the description of a material family but it can perform poorly for others. This drawback may be acceptable when one is interested in a given material. They exist, however, situations where a continuous variation of the material properties may produce hysteresis loops with broad range of features that cannot be captured by a single model.

This situation seems to be the case when we examine the magnetic hysteresis loops of cold rolled extra low carbon steels which are subjected to thermal annealing treatments. It turns out that the hysteresis loops of samples subjected to isothermal annealing at different temperatures and for different holding times, span a range of loop shapes, which is consequence of the different microstructural transformations that take place during the annealing processes.

Previous works have revealed that certain characteristics of the hysteresis loops, like the coercive field, the remanent magnetisation or the hysteresis losses correlate well with microstructural parameters like the grain size and the dislocation density and they can thus be used as identifiers for the evolution monitoring of transformation procedures such as the recovery and the recrystalisation [1, 2]. The thereupon presented results justify the need for numerical hysteresis models able of predicting the basic features of the hysteresis curves for the whole range of the family.

Numerical experimentation with existing parametric hysteresis models like the Jiles-Atherton model [3] or the Mel'gui model [4] revealed that the identification of the two models using a standard iterative optimisation procedure yields different results for the ensemble of the experimental curves obtained via the procedure described in [1, 2]. The reasons for these discrepancies may be attributed to the limitations of the models or even to the optimisation procedure itself, in the sense that regions with non-physical output for the model may be visited during the exploration of the input space.

To improve the precision of the representation, a mixing of the two models is proposed in this work. The main idea consists in sampling a common input space, consisting of characteristic hysteresis features like the ones mentioned above, and apply the best approach for each of the points of the input space based on a series of criteria concerning the form of the output curves. The sampling points are then used as training set for a Gaussian process regressor, which replaces the physical model thus becoming a generic hysteresis operator. In this way one can assure smooth variations across the input spaces and avoid "holes" with non-physical outputs. Although the physical parametric models considered here are the Jiles-Atherton and the Mel'gui model, the proposed approach is model independent making other combinations possible.

The paper is organised as follows. In the first section the Jiles-Atherton and the Mel'gui model and some rep-

resentative results of their identification for two different hysteresis loops are briefly presented. In the second section the hysteresis operator is reformulated in a more formal way, and the algorithm for the construction of the regressor model is presented. A brief presentation of the mathematical model of the Gaussian process regressor is given in the next paragraph. Details on the experimental procedure for the production of the material curves are provided in a separate section. The results of the approach for the reproduction of some representative experimental curves are presented at the last section.

2. Identification of the Jiles-Atherton and the Mel'gui model

In the Jiles-Atherton model [3] the total magnetisation of the material M is understood as the combined effect of two contributions: a reversible M_{rev}, related to the domain walls motion and an irreversible M_{irr} one, which is basically the result of the domain bulging. The two components are given by the equations

$$M_{rev} = c\,(M_{an} - M_{irr}) \tag{1}$$

and

$$\frac{M_{irr}}{dH} = \frac{M_{an} - M_{irr}}{k\delta/\mu_0 + \alpha\,(M_{an} - M_{irr})} \tag{2}$$

where c is a proportionality coefficient with $c \in [0, 1]$, μ_0 stands for the magnetic permeability of the free space, and k and α are material constants related to the domain wall pinning and the interdomain coupling, respectively. $\delta = \pm 1$ is essentially a numerical flag, which distinguishes between the descending and ascending branches. The M_{an} term stands for the anhysteretic material curve, calculated via the implicit relation

$$M_{an} = M_s L\left(\frac{H + aM_{an}}{a}\right) \tag{3}$$

with $L(x) = \coth(x) - 1/x$ being the Langevin function. M_s gives the magnetisation at saturation, and a is another material parameter related to the domains density.

In the Mel'gui model, the magnetisation is approximated by the following closed-form relation

$$\begin{aligned} M = \chi_{in}\frac{H_c^2 H}{H^2 + H_c^2} + \delta\frac{M_s}{\pi}\frac{H_m^2}{H_m^2 + bH_c^2} \\ \times \left\{2\arctan\left(\frac{H_c + \delta H}{H_0}\right)\right. \\ \left. - \left[\arctan\left(\frac{H_c + H_m}{H_0}\right) + \arctan\left(\frac{H_c - H_m}{H_0}\right)\right]\right\} \end{aligned} \tag{4}$$

with the coefficients H_0 and b being defined as

$$H_0 = \frac{H_c}{\tan(\pi M_r/2M_s)} \tag{5}$$

and

$$b = \frac{M_s}{\pi}\frac{\arctan(2H_c/H_0)}{M_c - \chi_{in}H_c/2}. \tag{6}$$

In the above equations, H_c, M_s, M_r stand for the coercive field, the magnetisation at the saturation and the remanent magnetisation respectively, χ_{in} is the initial susceptibility (susceptibility of the demagnetised state) and M_c the point of the first magnetisation curve at field intensity equal to the the coercive field.

The basic difference of the two models consists in the fact that whereas the magnetisation in the Jiles-Atherton model is obtained via the solution of an ordinary differential equation, in the Mel'gui model it is evaluated directly via a closed form relation, which makes the latter much faster. The domain of application is not the same either. Thus, the Jiles-Atherton model can theoretically be applied for an arbitrary excitation cycle (although the accuracy of the model for the description of minor loops is questionable), whereas the Mel'gui relation is only applicable to symmetrical periodic excitations. The input domain of the two models is also very different with four of the five parameters of the Jiles-Atherton model being internal tuning parameters that need to be determined via the so-called model identification procedure. The Mel'gui model, on the contrary, is parametrised via characteristic values of the major loop and the initial magnetisation curve, which makes the model directly applicable. Nevertheless, numerical experimentation reveals that the parameter estimation via identification (that is via the solution of an optimisation problem) yields better results for this model as well.

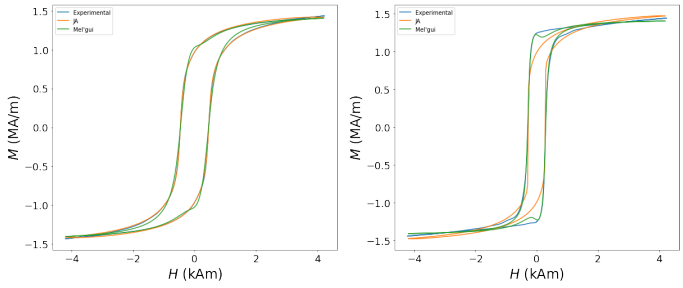

Figure 1: Hysteresis curves calculated using the Jiles-Atherton and Mel'gui model after identification with different experimental data. The experimental curves used for the identification are given for comparison.

An example of the two models identification using two different experimental curves with different coercivity is shown in Fig. 1. The models have been identified using a standard optimisation approach, where the L_2 norm of the residual between the theoretical and the experimental curve is minimized. It turns out that for the given minimisation procedure the Jiles-Atherton model performs slightly better than the Mel'gui model for the first curve (corresponding to a harder material) whereas the tendency is inverted for the second curve. As far as the second result is concerned, a possible explanation for the poor

performance of the Jiles-Atherton model could be that the utilised optimisation algorithm by trying to adapt the curve to the very steep slope around the coercive field does not succeed to fulfil all the rest of the form constrains at the same time. One must also not exclude the fact that regions with non-physical model solutions may be visited during the exploration of the input space, which destabilises the procedure and may lead to sub-optimal results.

3. Construction of the regressor model

3.1. Hysteresis description in different input spaces

The magnetisation for a scalar hysteretic magnetic material admits the general expression

$$M = M(H; H_0, H_{-1}, \ldots) \tag{7}$$

where H is the applied magnetic field at time t, and $H_{-r},\ r = 0, 1, \ldots$ stand for the field reversal points (i.e. the points where the time derivative of H changes sign) at previous instances $t_{-r} < t$. The value of the magnetic field H together with the ensemble of reversal points H_{-r} fully determine the state of the material taking full account of the excitation history.

Let us consider the hysteresis relation (7) along an observation window $t \in [0, T]$, which is sampled using a homogeneous temporal grid $t_i = iT/N$, with $i = 0, ..., N$. Assuming that the magnetic field values at the sample points of the observation window are known, the magnetic field vector $H_i = H(t_i)$ fully determines the magnetisation by application of (7) since H_i contains all the information of the field history (i.e. the reversal points H_{-r}).

We seek to establish the following mapping $\mathbf{H} \rightarrow \mathbf{M}$ with

$$\mathbf{M} = M(\mathbf{H})\,. \tag{8}$$

Notice that $\mathbf{H} = [H_0, \ldots, H_N]^T$ and $\mathbf{M} = [M_0, \ldots, M_N]^T$ stand here for column vectors comprising the values of the discretised magnetic field and magnetisation samples inside the observation window, which should not be confused with the vector counterparts of the two field variables.

We assume that a parametric model is used for the numerical evaluation of (8), which means that each pair $(\mathbf{H}, \mathbf{M})$ is associated to a set of parameters used for the tuning of the model of choice. Let $\mathbf{p}$ be the vector containing the values of the model parameters. One can formally write

$$\mathbf{M} = M_{\mathbf{H}}(\mathbf{p})\,, \tag{9}$$

where the index $\mathbf{H}$ is used to denote that the above mapping is valid for a given magnetic field discretisation $\mathbf{H}$. For the sake of notational simplicity, the model dependence on the $\mathbf{H}$ vector will be implied in the rest of the paper.

Our objective is to combine two (or more) different parametric models M_a and M_b into a common hysteresis operator, by either switching between the two models, interpolate between points calculated with the two models or by performing a weighted sum of their outputs. The three operations can be expressed in terms of a weighted sum

$$\mathbf{M} = w_a(\mathbf{p}_a)\, M_a(\mathbf{p}_a) + w_b(\mathbf{p}_b)\, M_b(\mathbf{p}_b)\,, \tag{10}$$

where $w_a(\mathbf{p}_a)$ and $w_b(\mathbf{p}_b)$ stand for the corresponding weighting coefficients, whose value vary between 0 and 1 depending on the given parameter combination. In order to build that operator, the input vectors of the two consisting models $\mathbf{p}_a$ and $\mathbf{p}_b$ must be expressed in a new parametric space, meaningful for both models.

The most straight-forward choice for this new space is to pick a number of hysteresis characteristic points or slopes, which are common features of all hysteresis curves and independent of the model details. A possible input set (among others) is the $\mathbf{p}_c = (M_s, H_c, M_r, W_h, \chi_r)$, where M_s is the magnetisation at saturation, H_c the coercive field, M_r the remanent magnetisation, W_h the hysteresis losses and χ_r the susceptibility at the remanence. We can rewrite then (10) formally in the following way

$$\mathbf{M} = w_a[\mathbf{p}_a(\mathbf{p}_c)]\, M_a[\mathbf{p}_a(\mathbf{p}_c)] + w_b[\mathbf{p}_b(\mathbf{p}_c)]\, M_b[\mathbf{p}_b(\mathbf{p}_c)]\,. \tag{11}$$

In order to proceed to the numerical evaluation of the scheme, one has to calculate the weighting coefficients $w_a(\mathbf{p}_c)$ and $w_b(\mathbf{p}_c)$ as functions of the new coordinates and to carry out the coordinate transformations $\mathbf{p}_a(\mathbf{p}_c)$ and $\mathbf{p}_b(\mathbf{p}_c)$. The algorithm of the regressor model is summarized in form of pseudo-code in the following table.

Algorithm 1 Regressor model

Off-line phase:

1: Define the domains $\mathbf{P}_a$, $\mathbf{P}_b$, with $\mathbf{p}_a \in \mathbf{P}_a$, $\mathbf{p}_b \in \mathbf{P}_b$
2: Random sampling of $\mathbf{p}_a$ and $\mathbf{p}_b$: get $\mathbf{p}_{a,i}$ and $\mathbf{p}_{b,i}$
3: **for** $i = 1 \ldots N_s$ **do**
4: Evaluate $M_a(\mathbf{p}_{a,i})$, $M_b(\mathbf{p}_{b,i})$
5: **if** $M_a(\mathbf{p}_{a,i})$, $M_b(\mathbf{p}_{b,i})$ non-physical **then**
6: Discard i
7: **else**
8: Evaluate the new coefficients $\mathbf{p}_{c,i} = \mathbf{p}_c(\mathbf{p}_{a_i}, \mathbf{p}_{b_i})$
9: Train the regressor $\mathscr{M}(\mathbf{p}_{c,i}) = w_a(\mathbf{p}_{a,i})\, M_a(\mathbf{p}_{a,i}) + w_b(\mathbf{p}_{b,i})\, M_b(\mathbf{p}_{b,i}) = \mathbf{M}_i$, $\forall i$

On-line phase:

1: Evaluate $\mathscr{M}(\mathbf{p}_c)$, with $\mathbf{p}_c \in \mathbf{P}_c$

For the case of the Jiles-Atherton and the Mel'gui model, which are the models of the choice in this work the two input vectors are $\mathbf{p}_a \equiv \mathbf{p}_{JA} = (M_s, k, a, \alpha, c)$ and $\mathbf{p}_b \equiv \mathbf{p}_{Mel} = (M_s, H_c, M_r, M_c, \chi_{in})$. A representative sampling of a $\mathbf{p}_c$ subspace is shown in Fig. 2, where the corresponding mapping from the Jiles-Atherton native parameter space $\mathbf{p}_{JA} \mapsto \mathbf{p}_c$ is also illustrated .

3.2. Hysteresis model based on Gaussian process regression

In the previous paragraph, a strategy of replacing the physical hysteresis model by a metamodel (regressor in this

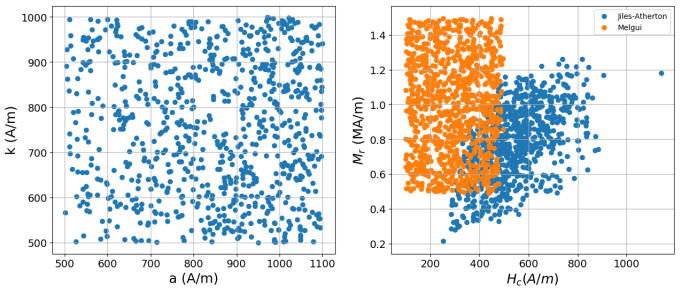

(a) (b)

Figure 2: Coordinate transformation. (a) Random sampling of the (a, k) subspace of the Jiles-Atherton native parameter space. (b) Sampling of the characteristics subspace $H_c - M_r$. With blue dots are marked the sampling points of the Jiles-Atherton model, given on the left figure, as they are transformed to the $H_c - M_r$ subspace. The orange points correspond to the sampling points of the Mel'gui model. Notice that the given subspace is a native subspace of the Mel'gui model (both H_c and M_r belong to its inputs).

case) built upon a number of pre-calculated data sets was presented. Very recently, different regression approaches based on metamodels have been studied in the literature of non destructive testing showing good accuracy in approximating unseen experimental data [5, 6]. Here we shall examine the case of the Gaussian process regression as it applies for the representation of hysteresis data.

Let us consider the hysteresis model sampled over a set of $\mathbf{P} = [\mathbf{p}_1, ..., \mathbf{p}_N]^{\mathrm{T}}$ parameters along with the respective –for sake of simplicity– scalar outputs $\mathbf{M}(\mathbf{p}_1), ..., \mathbf{M}(\mathbf{p}_N)$. Where the i-th entry $\mathbf{p}_i \in \mathbb{R}^{1\times P}$. Let us now consider the aforementioned outputs as a stochastic process where each entry is given by a random vector defined as $\mathscr{M} = (\mathscr{M}(\mathbf{p}_1), ..., \mathscr{M}(\mathbf{p}_N))$, where $\mathscr{M}$ stands for a random vector realisation. One can express the correlation between random variables as an exponential function with power equal to 2 which corresponds to the so-called Gaussian kernel function. Therefore, the correlation function calculated on the hysteresis model turns into

$$\phi(p_i, p_j) = \exp\left(-\sum_{p=1}^{P} \theta_j \left|\mathbf{p}_i - \mathbf{p}_j\right|^2\right), \qquad (12)$$

where θ_j is a hyper-parameter to be estimated via maximum likelihood estimation or cross validation methods. Starting from the definition of the correlation function between two random variables, one can show that the covariance matrix between these variables is given as $\mathrm{Cov}(\mathscr{M}, \mathscr{M}) = \sigma^2_{\mathscr{M}} \mathbf{\Phi}(\mathscr{M})$ [7] where $\mathbf{\Phi}$ being the $N \times N$ correlation matrix and $\sigma_{\mathscr{M}}$ is the standard deviation of $\mathscr{M}$. That is, the stochastic model considers the correlation between sampled data that can be accounted via a specific correlation model described by $\mathbf{\Phi}$. Therefore, the model depends on the distances between the considered sampled points. The Ordinary Kriging (OK) prediction ($\widehat{\mathscr{M}}(\cdot)$) on a new entry $\mathbf{p}_{N+1}$ is obtained by

$$\widehat{\mathscr{M}}(\mathbf{p}_{N+1}) = \sum_{p=1}^{P} \lambda_i \mathscr{M}(\mathbf{p}_i),$$

where λ_i are the kriging coefficients to be estimated [8]. Thus, accounting the unbiasedness of the predictions (i.e., $\widehat{\mathscr{M}}(\mathbf{p}_i) = \mathscr{M}(\mathbf{p}_i)$) leads to the following condition

$$\sum_{p=1}^{P} \lambda_i = 1,$$

which translates into the best linear unbiased prediction obtained by the minimisation of the mean square prediction error (i.e., the squared expectation) as [8]

$$\min_{\lambda_i} \mathbb{E}\left(\left[\widehat{\mathscr{M}}(\mathbf{p}_{N+1}) - \sum_{p=1}^{P} \lambda_i \mathscr{M}(\mathbf{p}_i)\right]\right)^2 \quad s.t. \sum_{i=1}^{P} \lambda_i = 1. \qquad (13)$$

The kriging coefficients in (13) can be obtained by applying the method of Lagrange multipliers. The optimisation boils down to the following matrix system of equations

$$\begin{bmatrix} \mathbf{\Phi} & \mathbf{U} \\ \mathbf{U}^{\mathrm{T}} & \mathbf{0} \end{bmatrix} \begin{bmatrix} \lambda \\ \mu \end{bmatrix} = \begin{bmatrix} \boldsymbol{\phi} \\ \mathbf{u} \end{bmatrix}, \qquad (14)$$

where in (14), $\mathbf{\Phi} = [\phi(\mathbf{x}_i, \mathbf{x}_j)]\ \forall i, j \in 1, ..., N$ and $\boldsymbol{\phi} = [\phi(\mathbf{x}_1, \mathbf{x}_{N+1}), \phi(\mathbf{x}_2, \mathbf{x}_{N+1}), ..., \phi(\mathbf{x}_N, \mathbf{x}_{N+1})]$ is defined as provided in (12). Moreover, $\mathbf{U} = \left[\mathbf{u}(\mathbf{p}_1)^{\mathrm{T}}, ..., \mathbf{u}(\mathbf{p}_N)^{\mathrm{T}}\right]^{\mathrm{T}}$ with $\mathbf{u}(\mathbf{p}_i)$ being a lower-order monomials (typically it does not exceed the degree of two), $\mathbf{0}$ is a zeros matrix and μ represents the vector of $l < N$ the Lagrange multipliers.

4. Application to microstructure monitoring during annealing treatment

4.1. Sample preparation and hysteresis measurements

Experimental magnetic measurements on cold rolled samples that had been annealed at low temperatures (300-500 °C) in order to promote recovery without interaction with recrystallisation and at 600 °C to induce recrystallisation were used in this study [1, 2]. The original samples were from extra low carbon steel, with composition 0.03%C-0.19%Mn-0.13%Al-0.0035%N-0.012%P-0.01%Si, that had been industrially produced and cold rolled to a final thickness of 0.3 mm through a reduction of 84% [1]. Near saturation major magnetic B-H hysteresis loop determination was made using a single sheet tester system available at CEIT [9] at 1 Hz, with maximum magnetic field strengths applied of about 4100 A/m. The schematic diagram of the B-H measurement system is shown in Fig. 3.

The external magnetic field was produced by a magnetic yoke composed of a 200-turn coil wound around a U-shaped magnetic laminated core. The excitation signal

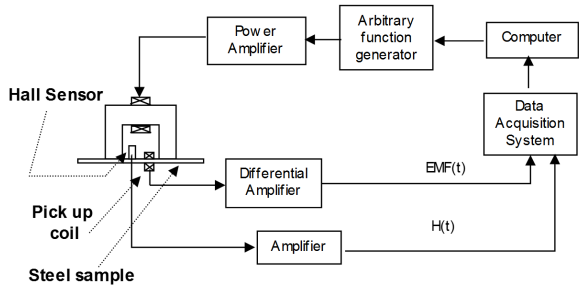

Figure 3: Experimental setup for the acquisition of the B-H curves.

was generated by a sinusoidal magnetizing current produced by a programmable function generator connected to a power amplifier. The induced electromotive force in an encircling coil wound around the samples and the tangential magnetic field strength measured using a Hall probe placed at the surface of the samples, were acquired using a NI data acquisition system.

Four major hysteresis loops were recorded for each measurement applying a sinusoidal magnetic field strength of about 4.1 kA/m at 1 Hz, which was sufficiently high to reach near saturation state of the measured samples. These were demagnetized prior to each test. The sampling frequency used was 5 kHz.

Recovery involves both the annihilation of dislocations and their rearrangement into low energy configurations. Recrystallisation leads to the suppression of dislocations by the nucleation of defect free volumes and by the migration through the material of the recrystallisation front, resulting in a new grain structure with a low dislocation density. Previous studies [1] showed that coercive field measurements can be satisfactorily employed to monitor recovery during low temperature annealing, during which the grain structure remains constant and microstructural changes only occur in the cold rolling dislocation substructure inside the grains. During recrystallisation both the effect of the reduction of the dislocation density and the change in the grain size have to be taken into account.

4.2. Identification of the regressor model using experimental data for different annealing conditions

The proposed approach has been applied for the reproduction of the experimental curves obtained from a cold-rolled (CR) low carbon (LC) steel sheets annealed at four different temperatures and for different holding times. Four temperatures are considered, namely 300 °C, 400 °C, 500 °C, and 600 °C. The annealing times for the four temperatures are given in Table 1. The predicted simulation curves are compared with the experimental ones for the four annealing temperatures in Fig. 4. It should be noticed at this point that a classical iterative Jiles-Atherton model identifications works very well for the curves of the lowest two temperatures, but it does not succeed to reproduce correctly the steeper ones obtained at 500 °C and 600 °C. This tendency is inverted in the case of the Mel'gui model,

Temperature	Annealing time
300 °C	51 s, 4 min, 12 min, 36 min, 1.2 h
400 °C	11 s, 51 s, 4 min, 12 min, 36 min, 1.2 h
500 °C	51 s, 4 min, 12 min, 36 min
600 °C	51 s

Table 1: Annealing conditions for the cold rolled steel samples.

which performs better for the steeper curves obtained at higher temperatures. A typical set of hysteresis characteristic features obtained for a selected set of four curves, one for each annealing temperature is given in Table 2.

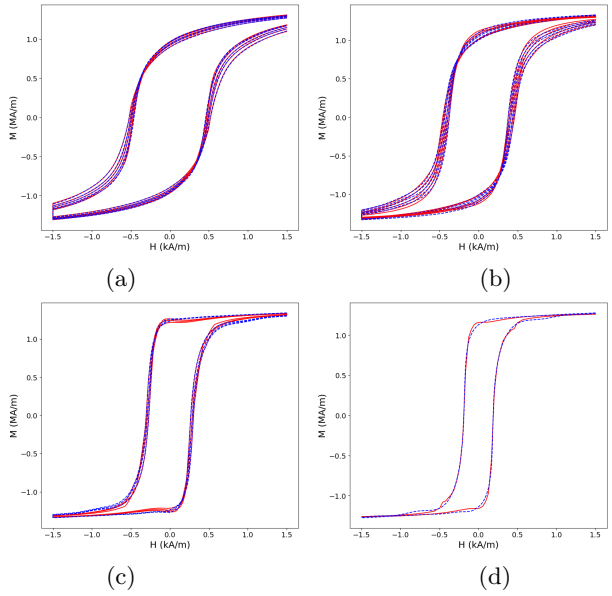

Figure 4: Experimental vs. simulated curves for the annealing conditions of Table 1. (a) 300 °C, (b) 400 °C, (c) 500 °C and (d) 600 °C. The experimental curves are drawn with dotted curves whereas the solid curves are the calculated hysteresis loops.

The two datasets used for the construction of the regressor, i.e. the datasets for the Jiles-Atherton and the Mel'gui model, contained 1803 and 1886 curves respectively. Each curve has been sampled using 600 points, which results in the storage of two databases of approximately 20 MB each. The construction of the regressor, which consists the most time consuming step, was carried out in 178 s. Once the regressor had been constructed, the identification of the four curves demonstrated in Fig. 4 was carried out in 3.18 s. The identification was based on five-parameters optimisation using the numpy python library implementation of the differential evolution algorithm. The average number of cost function evaluations needed to achieve the optimum was 2628, which results in an overhead per evaluation of circa 0.001 s. For the sake of comparison, it can be stressed out that the time demanded for a five-parameters optimisation using direct evaluation of the Jiles-Atherton model was of the order of 130 s. Both calculations were carried out in a standard DELL Precision T1700 workstation with an Intel Xeon CPU E3-1241 v3 and 16 Gbytes

RAM. This drastic reduction of the computational time can be attributed to the very fast evaluation of each candidate curve via the regression approach (in fact we interpolate in a set of pre-calculated curves), and constitutes one of the major advantages of the proposed approach.

The H_c vs. M_r and H_c vs. W_h correlation plots deliver important information about the metalurgical transformation, which makes them a further test for the performance of the regressor. The correlation plots for the calculated curves are shown in Fig. 5. It is important to notice that both pairs demonstrate a linear correlation for the first three temperatures, which is the trend observed using the experimental data [1, 2]. A slight deviation from the strict linear law is observed at the H_c–W_h plot for the last three points (longer annealing) of the third temperature. The point corresponding to the 600 °C curve does clearly fall apart, which is explained by the fact that at this point the recrystallisation is activated, when additionally to the effect of the reduction of the dislocation density, an additional effect of the variation of the grain size takes place [2, 10].

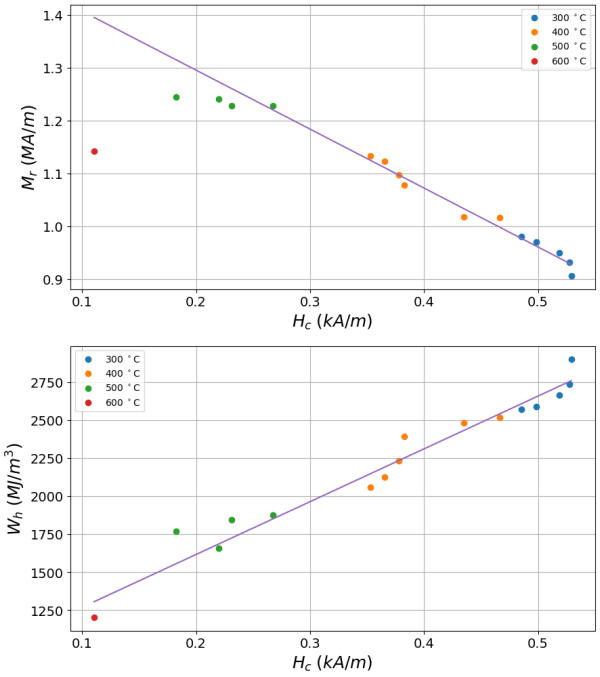

Figure 5: Correlation of the remanent magnetisation and the hysteresis losses with the coercive field. a) H_c vs. M_r , (b) H_c vs. W_h.

Conclusions

A regressor-based hybridisation of two parametric models has been proposed in order to describe sets of experimental curves with a broad range of features. The present work follows a procedure, where the physical hysteresis model is replaced by a generic meta-model, a similar idea to the one previously exploited in [11].

The use of the regressor presents a number of advantages, when a pragmatic approach is sought in order to reproduce experimental data with a reasonable accuracy. The computationally expensive model identification (i.e. the calculation of the model parameters via fitting to the experimental curve), is significantly accelerated since each call to the physical model is replaced by a regressor evaluation, which is carried out in nearly real time. This acceleration, also discussed in [11], is particularly interesting with models like the Jiles-Atherton model, where the evaluation of a curve signifies the solution of a differential equation. Furthermore, the above adopted approach stabilises the identification procedure. This can be understood by pointing the fact that the minimisation algorithm (which can be either a deterministic conjugate-gradient-based algorithm or a stochastic approach like evolutionary or genetic algorithms) may enter in domains where the physical model yields unphysical solutions. This problem is avoided by the selection taking place in the off-line phase of the regressor construction. Finally, the fact that the approach is not depending on model-specific variables (the regressor is trained using input-output pairs) allows the mixing of more than one physical models, and the extension of the domain of validity of each one of them.

Although two particular physical models have been considered in this work, namely the Jiles-Atherton and the Mel'gui model, the approach is general and can be applied with an arbitrary combination of models.

References

[1] A. Martínez-de-Guerenu, F. Arizti, M. Díaz-Fuentes, I. Gutiérrez, Recovery during annealing in a cold rolled low carbon steel. Part I: Kinetics and microstructural characterization, Acta Mater. 52 (12) (2004) 3657–3664. doi:10.1016/j.actamat.2004.04.019.

[2] A. Martínez-de-Guerenu, K. Gurruchaga, F. Arizti, Non-destructive characterization of recovery and recrystallization in cold rolled low carbon steel by magnetic hysteresis loops, J. Mag. Mag. Mater. 316 (2) (2007) e842–e845. doi:10.1016/j.jmmm.2007.03.110.

[3] D. C. Jiles, D. L. Atherton, Theory of ferromagnetic hysteresis, J. Mag. Mag. Mater. 61 (1986) 48–60. doi:10.1016/0304-8853(86)90066-1.

[4] M. A. Mel'gui, Formulas for describing nonlinear and hysteretic properties of ferromagnets, Defektoskopiya 11 (1987) 3–10, (Translated from rusian).

[5] M. Salucci, N. Anselmi, G. Oliveri, P. Calmon, R. Miorelli, C. Reboud, A. Massa, Real-time NDT-NDE through an innovative adaptive partial least squares SVR inversion approach, IEEE Trans. Geosci. Remote Sens. 54 (11) (2016) 6818–6832. doi:10.1109/TGRS.2016.2591439.

[6] S. Ahmed, C. Reboud, P.-E. Lhuillier, P. Calmon, R. Miorelli, An adaptive sampling strategy for quasi real time crack characterization on eddy current testing signals, NDT & E Int. 103 (2019) 154–165. doi:10.1016/j.ndteint.2019.02.001.

[7] A. Forrester, A. Sobester, A. Keane, Engineering design via surrogate modelling: a practical guide, John Wiley & Sons, 2008.

[8] J. Villemonteix, E. Vazquez, E. Walter, An informational approach to the global optimization of expensive-to-evaluate functions, Journal of Global Optimization 44 (4) (2008) 509–534. doi:10.1007/s10898-008-9354-2.

Annealing conditions	H_c (A/m)	W_h (MJ/m^3)	M_r (MA/m)	M_s (MA/m)	χ_r
300 °C, 51 s	529.1	2901.6	0.905	1.418	636.8
400 °C, 51 s	434.6	2479.9	1.017	1.434	673.7
500 °C, 51 s	267.2	1875.1	1.228	1.368	896.7
600 °C, 51 s	110.5	1199.6	1.142	1.291	984.4

Table 2: Hysteresis features obtained after fitting to the experimental curves corresponding to 51 s isothermal annealing at the four different considered temperatures.

[9] M. Soto, A. Martínez-de-Guerenu, K. Gurruchaga, F. Arizti, A completely configurable digital system for simultaneous measurements of hysteresis loops and barkhausen noise, IEEE Trans. Instrum. Meas. 58 (5) (2009) 1746–1755. doi:10.1109/TIM.2009.2014510.

[10] K. Gurruchaga, A. Martínez-de-Guerenu, I. Gutiérrez, Sensitiveness of magnetic inductive parameters for the characterization of recovery and recrystallization in cold-rolled low-carbon steel, Metall. Mater. Trans. A 41A (2010) 985– 993. doi:10.1007/s11661-009-0156-z.

[11] A. Skarlatos, A. Martínez-de Guerenu, R. Miorelli, A. Lasaosa, C. Reboud, Use of meta-modelling for identification and interpolation of parametric hysteresis models applied to the characterization of carbon steels, Physica B 549 (2018) 122–126. doi:10.1016/j.physb.2017.11.053.